Pure Appl. Chem., Vol. 76, No. 1, pp. 49–61, 2004.

Solid-state proton conduction: An ab initio molecular dynamics investigation of ammonium perchlorate doped with neutral ammonia*

Lula Rosso[1] and Mark E. Tuckerman[2,‡]

[1]*Department of Chemistry, New York University, New York, NY 10003, USA;*
[2]*Department of Chemistry and Courant Institute of Mathematical Sciences, New York University, New York, NY 10003, USA*

Abstract: The charge-transport mechanism in solid ammonium perchlorate crystal exposed to an ammonia-rich environment is studied using ab initio molecular dynamics. Ammonium perchlorate is an ionic crystal composed of NH_4^+ and ClO_4^- units that possesses an orthorhombic phase at $T < 513$ K and a cubic phase at $T > 513$ K. Exposure to an ammonia-rich atmosphere allows ammonia molecules to be absorbed into the crystal at interstitial sites. It has been proposed that these neutral ammonias can form short-lived $N_2H_7^+$ complexes with the NH_4^+ ions allowing proton transfer between them, thereby enhancing the conductivity considerably. To date, however, there has been no direct evidence of this proposed mechanism. In this paper, ab initio molecular dynamics techniques are employed to explore this mechanism. By comparing computed infrared spectra of the pure and ammonia-doped crystals, we observe a significant broadening of the NH stretch peak into a lower frequency region, indicating through an experimentally verifiable observable, the formation of hydrogen bonds between NH_3 and NH_4^+ units. This suggestion is confirmed by direct observation of $N_2H_7^+$ complexes from the trajectory. Comparison of the diffusion constants of NH_4^+ in the pure and doped crystals yields a ratio that is comparable to the experimentally measured conductivity ratio and clearly shows an enhanced positive charge mobility. Finally, compelling evidence suggesting the possibility of an ammonia umbrella inversion following proton transfer from NH_4^+ and NH_3 is obtained.

INTRODUCTION

Solid-state proton conductors are systems of considerable importance because of their potential uses in solid-state batteries, sensors, and other electrochemical devices. For this reason, there is a growing interest in such systems. However, unlike in aqueous electrolyte solutions, where proton transfer steps occur readily due to anomalous mechanisms [1–5], proton transfer reactions in many crystalline systems are rare processes. Hence, proton conducting solids are of particular scientific interest because of their novelty. Indeed, a particular class of materials, proton conducting molecular crystals, has received considerable attention because of their wide range of structural and dynamical characteristics. A variety of such crystals can undergo temperature- and/or pressure-induced structural phase transitions, and, in some cases, thermal decomposition may occur with a concomitant release of a large amount of en-

*Lecture presented at the European Molecular Liquids Group (EMLG) Annual Meeting on the Physical Chemistry of Liquids: Novel Approaches to the Structure, Dynamics of Liquids: Experiments, Theories, and Simulation, Rhodes, Greece, 7–15 September 2002. Other presentations are published in this issue, pp. 1–261.
‡Corresponding author

ergy. One such material that has been studied extensively is the ammonium salt crystal, ammonium perchlorate (NH_4ClO_4) [6–23].

Ammonium perchlorate (AP) is one of the showcase examples of thermally labile material that can undergo a decomposition process at high temperature, leading to its use in applications such as rocket propulsion (see, e.g., the discussion in Oxtoby and Nachtrieb's *Principles of Modern Chemistry* [24]). The crystal structure of AP is temperature-dependent: at temperatures below 513 K, it possesses an orthorhombic unit cell with space group *Pnma*, while at temperatures above 513 K, it undergoes a structural phase transition to a simple cubic structure with space group $T_d^2 - F\bar{4}3m$. While particular attention has been devoted to the electrical conductivity of AP, the microscopic mechanism of charge transfer has never been satisfactorily elucidated. Currently, two schools of thought prevail. One interpretation of conductivity measurements is that a protonic defect can be formed in which ammonium (NH_4^+) ions transfer an excess proton to nearby perchlorate anions. This mechanism has also been implicated as important in the initial stages of thermal decomposition [8,9,15], although more recent experiments favor an electron-transfer process [19]. In the high-temperature phase, it is thought that the perchlorate (ClO_4^-) anions can undergo "nearly free" rotation, which presumably allows $HClO_4$ units to move protons to other NH_3 defects. However, another interpretation, based on comparative studies of the conductivity of AP and rubidium perchlorate, suggests a purely diffusive mechanism in which relatively mobile NH_4^+ units diffusive through a "matrix" of slowly rotating ClO_4^- ions. The latter of these appears to be supported by infrared and Raman spectroscopic measurements [6,17], which indicate that the ammonium ion, itself, undergoes nearly free rotation (estimates of the barrier range from 0.5 to 1.0 kcal/mol [13,17,16]). This finding suggests that interactions between the NH_4^+ and ClO_4^- ions are relatively weak, which supports the notion that diffusion of NH_4^+ ions along crystalline planes is possible.

Additional experiments on AP crystals [12] indicate that the electrical conductivity of AP increases markedly when it is exposed to an ammonia-rich atmosphere. Based on these findings, it has been suggested that the increased conductivity is due to an anomalous Grotthuss-type mechanism in which the mobile NH_4^+ ions can transfer protons to the neutral ammonia molecules at lattice vacancies or at interstitial sites. The newly formed neutral ammonia molecules at lattice sites subsequently become recipients of excess protons from NH_4^+ ions now at interstitial sites. This mechanism is expected to dominate over the formation of Schottky or Frenkel defects [12]. However, the suggestion of such a process leaves many microscopic-level questions unanswered, and, indeed, the increased conductivity cannot be regarded as definitive evidence of the truth of such a mechanism.

Given the many unanswered questions concerning charge transport in AP crystal and the general importance of solid-state proton conduction, we have undertaken an ab initio molecular dynamics (AIMD) study of ion rotation and charge transport in AP crystal in both its low (orthorhombic) and high (cubic) temperature phases. In these studies, finite-temperature molecular dynamics trajectories are generated with forces determined directly from electronic structure calculations performed "on the fly" as the simulation proceeds via the Car–Parrinello approach [25]. The electronic structure is described by a gradient-corrected density functional theory (DFT) representation. The validity of the DFT approach in ammonia systems, including the pure liquid [26,27] and ion solvation in the liquid [27] has been previously verified. Direct access to the electronic properties of the system allows the infrared (IR) spectra of the two phases of the crystal to be computed and compared to experiment. Moreover, calculation of the IR spectrum of AP with neutral ammonia placed in interstitial sites at a mole fraction of 0.5 [to be denoted hereafter as $AP{\cdot}(NH_3)_{0.5}$] provides direct, experimentally verifiable evidence of the formation of relatively short-lived hydrogen-bonded $N_2H_7^+$ complexes through which a proton can be transferred from NH_4^+ to NH_3. That such transfers are possible has been suggested by numerous gas-phase studies of the $N_2H_7^+$ complex [27–32].

The signals in the IR spectrum indicative of the formation of such complexes are a strong red-shift in the NH stretch band and a broadening of this band, both being caused by strong hydrogen bond-

ing between NH_4^+ and NH_3. The presence of $N_2H_7^+$ complexes in the doped crystal is also confirmed by direct observation from the trajectories. In addition, the ratio of calculated diffusion constants of NH_4^+ in the pure AP and the AP·$(NH_3)_{0.5}$ crystals is consistent with the ratio of the measured conductivities. As no proton transfer between the NH_4^+ and ClO_4^- ions in the pure AP crystal is observed on the time scale of our MD simulations in either the orthorhombic or cubic phases, we propose that the dominant charge-transport mechanism in pure AP crystal is diffusion of the NH_4^+ ions in particular crystal planes. Consistent with the observed rotational behavior of the ClO_4^- ion [17], we also find a marked increase in the rotation rate of ClO_4^- in the cubic phase over the orthorhombic phase. Finally, the simulations yield compelling evidence of the possibility of umbrella inversion events of newly formed NH_3 in the doped crystal following the proton-transfer step.

METHODOLOGY

AIMD simulations of the AP crystal in the low-temperature orthorhombic and high-temperature cubic phases were carried out using the Car–Parrinello extended Lagrangian method [25]. In the orthorhombic phase, whose space group is D_{2h}^{16} – *Pbnm* (= *Pnma*) [33–35], two unit cells were used, giving a supercell with dimensions L_x = 9.2 Å, L_y = 11.6 Å, and L_z = 7.45 Å to which periodic boundary conditions were applied. Two unit cells in the cubic phase, whose space group is T_d^2 – $F\bar{4}3m$ [36], were used as well, giving a periodic supercell with dimensions, L_x = 15.2598 Å, L_y = 7.6299 Å, and L_z = 7.6299 Å. In addition to the pure crystal, trajectories were also generated for an AP crystal doped with neutral NH_3 molecules placed at interstitial sites in the high-temperature cubic phase at a mole fraction of approximately 0.5. Simulations were also carried out for supercells consisting of 4 unit cells, for which the box dimensions were L_x = 15.2598 Å, L_y = 15.2598 Å, and L_z = 7.6299 Å. In all cases, the electronic structure was represented within the generalized gradient approximation (GGA) of density functional theory (DFT) using the B-LYP functional [37,38]. The Kohn–Sham orbitals were expanded in a plane-wave basis up to a cutoff of 70 Ry, and core electrons were replaced by atomic pseudopotentials of the Troullier–Martins form [39] for nitrogen, oxygen, and hydrogen and of the Gödecker et al. type for chlorine [40,41]. This simulation protocol has been shown to reproduce well the experimental radial distribution functions in liquid ammonia (see Fig. 1) [42]. In the low-temperature calculations, the system was equilibrated for 1 ps under NVT conditions at a temperature of 300 K using a Nosé–Hoover chain thermostat [43] and then allowed to run under microcanonical conditions for 10 ps. In the high-temperature case, the system was equilibrated for 3 ps under NVT conditions at a temperature of 530 K and then allowed to evolve under microcanonical conditions for 15 ps. In the AP·$(NH_3)_{0.5}$ system with two unit cells, an equilibration stage at 530 K of 5 ps was followed by a production run of 27 ps, while in the four-unit cell case, equilibration of 1.5 ps at the same temperature was followed by a production run of 17 ps. In all cases, a time step of 0.12 fs was used. All calculations were performed using the CPMD [44] and PINY MD [45] codes.

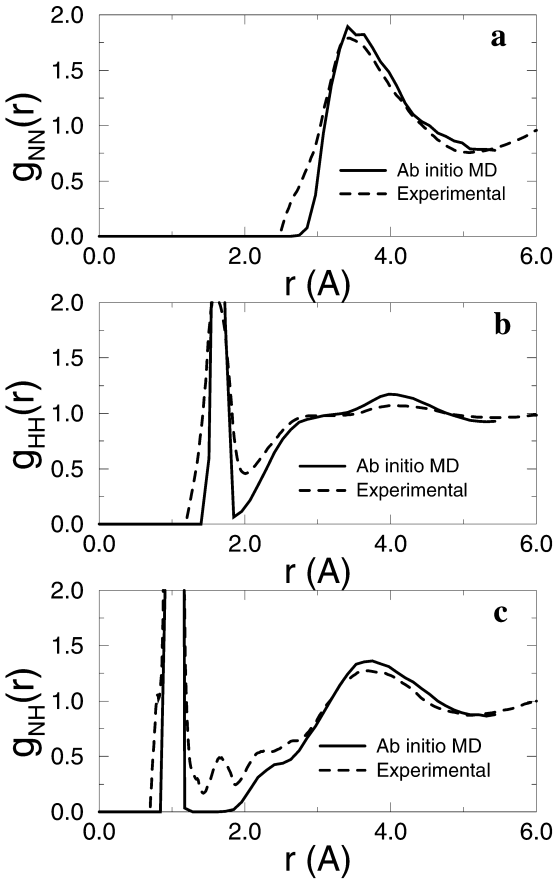

Fig. 1 Comparison of calculated (solid line) and experimental (dashed line) [42] radial distribution functions for pure liquid ammonia: (a) nitrogen–nitrogen, (b) hydrogen–hydrogen, and (c) nitrogen–hydrogen.

RESULTS AND DISCUSSION

Infrared spectra

The procedure for calculating the IR spectrum in an ab initio MD simulation is described in detail elsewhere [46–50]. Here, we briefly review the technique. The IR absorption coefficient, $\alpha(\omega)$, at frequency ω can be computed using linear response theory from the autocorrelation function of the total electric dipole moment, $\mathbf{M}(t)$, via [51]

$$\alpha(\omega)n(\omega) = \frac{4\pi\omega \tanh(\beta\hbar\omega/2)}{3\hbar cV} \int_{-\infty}^{\infty} dt\, e^{-i\omega t} \langle \mathrm{M}(t) \cdot \mathrm{M}(0) \rangle \tag{1}$$

where $n(\omega)$ is the refractive index, c is the speed of light in vacuum, V is the system volume, and $\beta = 1/k_{\mathrm{B}}T$. The total dipole moment consists of both ionic and electronic contributions. While the former can be computed straightforwardly, the latter cannot because the quantum mechanical position operator is not well defined for an infinite periodic system [47,49,50]. This difficulty has been solved using the so-called Berry phase approach [46,47,49,50] according to which the electronic contribution to the dipole moment for a cubic supercell at the Γ-point is given by

$$M_{\mathrm{elec}}^{(\gamma)} = -\frac{eL}{\pi} \mathrm{Im\ ln\ det} \left[\mathrm{R}^{(\gamma)} \right] \tag{2}$$

where γ indexes the three spatial components, and the matrix $R^{(\gamma)}$ is given by

$$R_{ij}^{(\gamma)} = \left\langle \Psi_i \left| e^{-2\pi i r_\gamma / L} \right| \Psi_j \right\rangle \tag{3}$$

Here, $r_\gamma = x,y,z$ for $\gamma = 1,2,3$, respectively and $|\Psi_i\rangle$ is the ith Kohn–Sham orbital. In general, run lengths are too short to compute the IR spectrum by direct Fourier transformation of the autocorrelation function. In this case, maximum entropy methods [52] can be very useful as a means of extracting the spectrum, as we have shown in previous calculations in high- and low-concentration KOD solutions [53]. In the present case, a maximum entropy method based on the 200-point Burg algorithm [52] was employed. As always with maximum entropy methods, one needs to check that a given order algorithm does not introduce spurious features into the spectra. In the present case, the computed spectra were checked and were not found to be sensitive to the order of the maximum entropy algorithm—essentially the same result was obtained with 150, 200, 250, and 300 points.

The IR spectrum for the low-temperature orthorhombic phase is shown in Fig. 2a. The inset shows the experimental spectrum [6,16]. As can be seen from the figure, good agreement is obtained between the experimental and computed spectra. The broad band at 3150 cm^{-1} corresponds to the NH stretch modes. This serves as a benchmark for the present AIMD protocol. In Fig. 2b, the IR spectra for the pure AP and AP·$(NH_3)_{0.5}$ systems in the cubic phase are shown together. The AP·$(NH_3)_{0.5}$ spectrum corresponds to the system with 2 unit cells. In Fig. 2c, a comparison of the spectra between 2 and

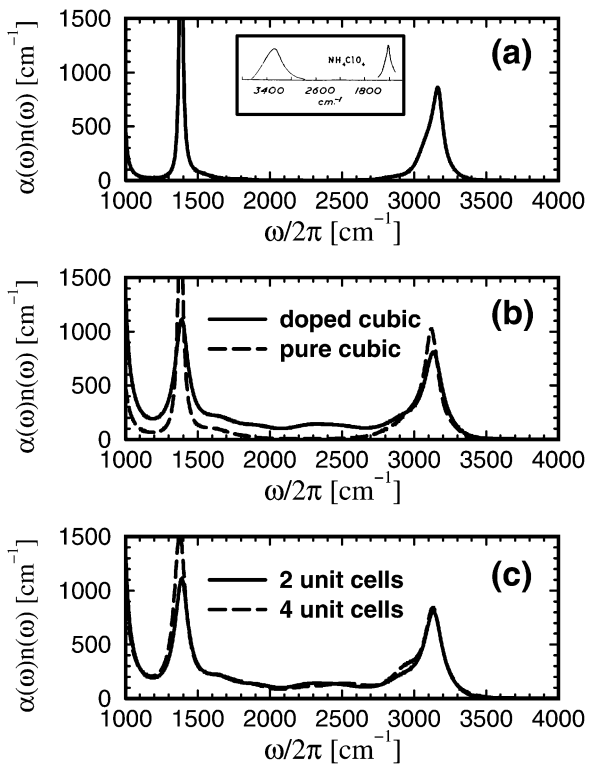

Fig. 2 (a) Infrared spectrum for pure ammonium perchlorate crystal in the orthorhombic phase at 300 K. The inset shows the experimental spectrum from ref. [1]. (b) Infrared spectra for ammonium perchlorate in the cubic phase at 530 K. The dashed line shows the spectrum for the pure crystal, and the solid line shows the spectrum for the ammonia-doped crystal. (c) Infrared spectra for 2 (solid line) and 4 (dashed line) unit cells of ammonia-doped ammonium perchlorate crystal in the cubic phase at 530 K.

4 unit cells of the AP·$(NH_3)_{0.5}$ system is shown. In Fig. 2b, it can be seen that in the AP·$(NH_3)_{0.5}$ spectrum, the NH stretch band is broadened to the left, indicating a red-shift of some of the NH stretch modes. We interpret this finding as a clear signal of the formation of strongly hydrogen-bonded $N_2H_7^+$ complexes. In recent DFT-based studies of proton transfer in the $N_2H_7^+$ complex at 300 K [27], a very small free-energy barrier to proton transfer (0.3–0.5 kcal/mol) was obtained, indicating a relatively strong hydrogen bond between NH_4^+ and NH_3. Such strong hydrogen bonds generally cause a red-shift of the NH stretch frequencies in IR spectra, as Fig. 2b clearly shows. In order to check the dependence of the barrier height on temperature, we carried a similar study of the gas-phase $N_2H_7^+$ complex at a temperature of 530 K using the same DFT scheme and simulation protocol as for the crystal. The resulting free-energy profile is shown in Fig. 3a, together with the profile from ref. 24. The reaction coordinate in this case is taken to be proportional to the asymmetric stretch of the proton:

$$\delta = d_{N_1H^*} - d_{N_2H^*} \tag{4}$$

where $d_{N_iH^*}$ is the distance of the shared proton, H* from nitrogen, N_i, i = 1,2. It can be seen that that there is only a relatively small barrier at both high and low temperatures. Finally, in Fig. 2c, the comparison of spectra for 2 and 4 unit cells of the AP·$(NH_3)_{0.5}$ system shows the spectra for the two system sizes are very similar, indicating that finite size effects are of minor importance for the IR spectra.

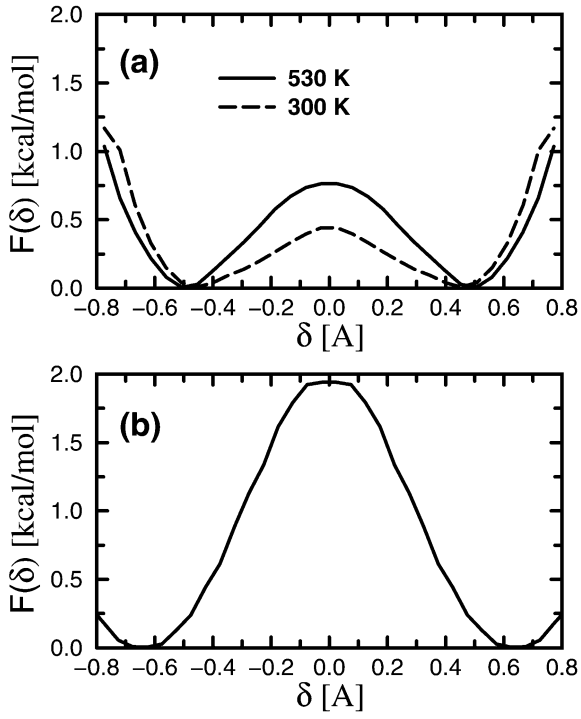

Fig. 3 (a) Proton-transfer free-energy profiles as a function of the reaction coordinate, δ (cf. eq. 4) for the $N_2H_7^+$ complex in the gas phase at 300 K (dashed line) and at 530 K (solid line). (b) The same in the cubic phase of the ammonia-doped ammonium perchlorate crystal at 530 K.

Charge transport

The spectra of the previous section provide strong evidence of the formation of $N_2H_7^+$ complexes in the AP·$(NH_3)_{0.5}$ system. Moreover, gas-phase studies at 300 and 530 K of the $N_2H_7^+$ complex indicate that

proton transfer through the N-H···N hydrogen bond is possible. In this section, we present further evidence from the simulations that the charge-transport mechanism in the AP·$(NH_3)_{0.5}$ is dominated by such proton-transfer steps. In Fig. 4a, radial distribution functions in the pure AP and AP·$(NH_3)_{0.5}$ systems in the high-temperature cubic phase. In the AP·$(NH_3)_{0.5}$ system, the presence of a peak at 2.7 Å provides further evidence of the formation of $N_2H_7^+$ complexes. Interestingly, this value is similar to that obtained in recent studies of stabilization of the $N_2H_7^+$ complex in the supramolecular calix[4]arene$^-$ anion cavity [54] and the value 2.9 Å of the NN distance between NH_4^+ and NH_3 when the former is solvated in liquid ammonia [27]. This value should also be compared with the average nitrogen–nitrogen distance in the pure crystal, 4.6 and 4.7 Å, in the orthorhombic and cubic phases, respectively. Visual inspection of the trajectories shows that these complexes play a critical role in the charge transport process. Because of the relatively high mobility of both the NH_4^+ and NH_3 units in the system, $N_2H_7^+$ complexes of finite lifetime are formed. While these complexes live, the proton can be transferred from NH_4^+ to NH_3. If the complex dissociates after the proton has been transferred, the result is a neutral NH_3 at a lattice site and an NH_4^+ at an interstitial site. In this state, the neutral NH_3 is able to accept another proton from a nearby NH_4^+, leading to a kind of "relay" mechanism based the formation and dissociation of $N_2H_7^+$ complexes. The free-energy profile associated with the proton-transfer process, characterized by the reaction coordinate of eq. 4, is shown in Fig. 3b together with the gas-phase free-energy profile at 530 K. The figure shows that the barrier to proton transfer is higher (~2 kcal/mol) than in the gas phase, but is still relatively low.

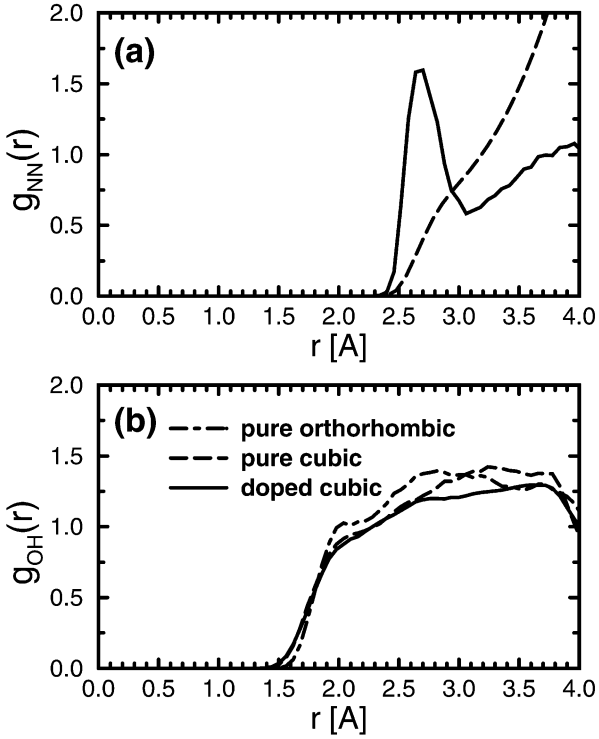

Fig. 4 (a) The nitrogen–nitrogen radial distribution function (solid line) in the cubic phase of the ammonium-doped ammonium perchlorate crystal at 530 K. The dashed line shows the integrated coordination number. (b) Oxygen–hydrogen radial distribution functions in the cubic phase of pure (dashed line) and ammonia-doped (solid line) ammonium perchlorate crystals.

In order to quantify the enhancement in charge transport in the AP and AP·$(NH_3)_{0.5}$ crystals, the mean-square displacements of the NH_4^+ units in both systems are plotted in Fig. 5a. The figure shows a dramatic enhancement in the rate of diffusion of positive charge carriers in the AP·$(NH_3)_{0.5}$ crystal. From the slopes of the linear part of these curves, we find that the ratio of diffusion constants is approximately 4.9. This number is very similar to the measured conductivity ratios 4.5 and 6.0 at mole fractions 0.42 and 0.61, respectively at 503 K [7]. Although these quantities are not directly comparable, the fact that they are in the same range leads to an important prediction concerning charge transport in the pure AP crystal in its high-temperature phase. First, consider the OH radial distribution functions of AP in the orthorhombic and cubic phases shown in Fig. 4b. These show that the ammonium and perchlorate units are never close enough (on the time scale of the present simulations) to allow proton transfer from NH_4^+ to ClO_4^-, indicating that such a process would be a very rare event. Based on this finding and the computed diffusion constant ratio, we conjecture that the charge-transport mechanism in pure AP crystal in both the cubic and orthorhombic phases is dominated by diffusion of the NH_4^+ ions. Indeed, from the free-energy profile of NH_4^+ rotation (not shown), we estimate a rotational barrier of no more than a few tenths of a kcal/mol, in agreement with experimental estimates [13,17,16], which suggests only weak interactions between the NH_4^+ and ClO_4^- units. Also shown in Fig. 5b are the mean-square displacement curves for the ClO_4^- ions in the orthorhombic and cubic phases. Comparison of these figures shows that in the pure crystal, somewhat contrary to the common conception, the NH_4^+ and ClO_4^- ions actually diffuse at roughly the same rate, while in the AP·$(NH_3)_{0.5}$ crystal, the charge-transport process occurs in a slowly moving background matrix of ClO_4^- ions. This suggests that, in the pure crystal, motion of NH_4^+ is limited by the slower diffusion of ClO_4^-.

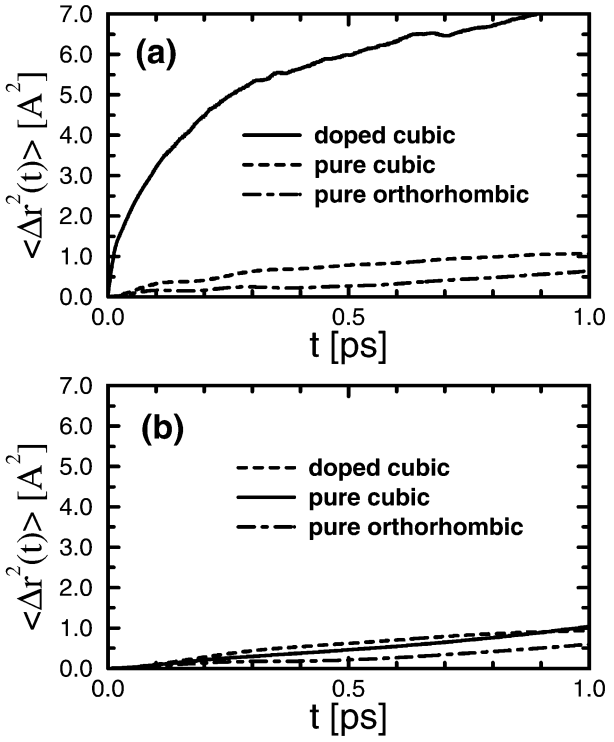

Fig. 5 (a) Mean-square displacements of NH_4^+ in the pure orthorhombic ammonium perchlorate crystal at 300 K (dashed–dotted line), pure cubic ammonium perchlorate crystal at 530 K (dashed line), and doped cubic ammonium perchlorate crystal at 530 K (solid line). (b) The same for the ClO_4^- anion.

Ion rotation

Further information about the dynamics of the AP and AP·$(NH_3)_{0.5}$ crystals can be gleaned from a study of rotation of the NH_4^+ and ClO_4^- ions. It has been proposed that the ClO_4^- ions have greater rotational freedom in the high-temperature cubic phase than in the orthorhombic phase, while the NH_4^+ ions can undergo "nearly free" rotation in both phases. Moreover, if directional bonding with neutral ammonias in the AP·$(NH_3)_{0.5}$ crystal plays such an important role in the charge-transport process, as discussed in the previous subsection, then it should be possible to detect a suppression of such nearly free rotation of the NH_4^+ ion in the AP·$(NH_3)_{0.5}$ system. To this end, we plot, in Figs. 6a and 6b, the rotational mean-square displacements of the NH_4^+ and ClO_4^- ions, respectively, in the orthorhombic and cubic phases of pure AP crystal and of the AP·$(NH_3)_{0.5}$ system. These are expressed as

$$\Delta\mathbf{u}^2(t) = \left\langle \frac{1}{N^*} \sum_{i=1}^{N^*} \left[\hat{\mathbf{u}}_i(t) - \hat{\mathbf{u}}_i(0)\right]^2 \right\rangle \tag{5}$$

where $\hat{\mathbf{u}}_i(t)$ is the unit vector along the bond from a central atom (Cl for ClO_4^- and N for NH_4^+ ions, respectively) to atoms bond to it (O for ClO_4^- and H for NH_4^+, respectively), and the sum, with $N^* = 4$, runs over the four O or H atoms in each case. The figure shows that the ClO_4^- ion rotation exhibits diffusive behavior in the cubic phase, while in the orthorhombic phase, the rotational motion is severely hindered. In addition, it can be seen that rotational diffusion of NH_4^+ is comparable in the orthorhombic and cubic phases, but that there is a slight suppression of rotation in the AP·$(NH_3)_{0.5}$ system. This latter finding provides further evidence of the formation of hydrogen-bonded $N_2H_7^+$ complexes.

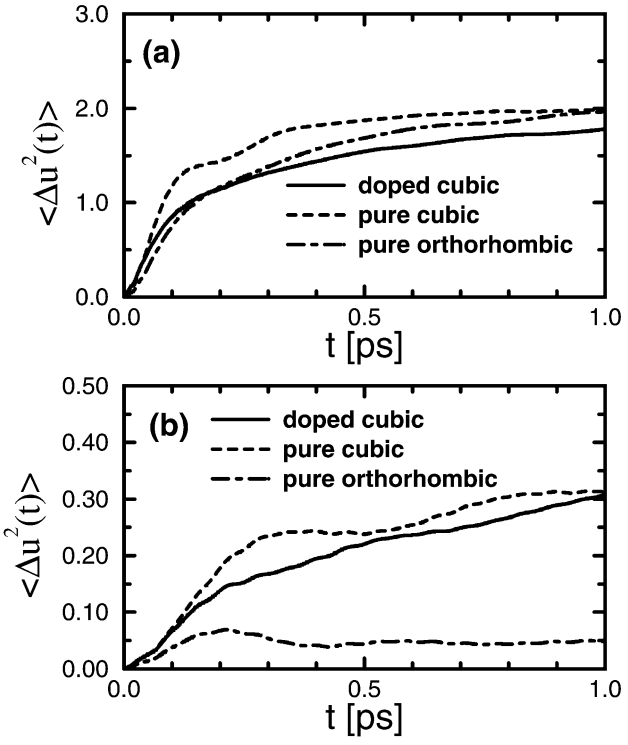

Fig. 6 (a) Rotational mean-square displacement curves as defined by eq. 5 for the NH_4^+ cation in the pure orthorhombic ammonium perchlorate crystal at 300 K (dashed–dotted line), pure cubic ammonium perchlorate crystal at 530 K (dashed line), and doped cubic ammonium perchlorate crystal at 530 K (solid line). (b) Same for the ClO_4^- anion. Note the difference in the scale on the *y*-axis.

Ammonia rotation vs. umbrella inversion

Once an NH_4^+ ion transfers a proton to a neutral NH_3, the newly created NH_3 is not in a correct orientation to accept a proton from a different NH_4^+. In particular, the NH_3 either needs to rotate in such a way that its lone pair points in the opposite direction along the C_3 axis compared to its configuration just after proton transfer, or it must undergo an umbrella inversion so as to leave the NH_3 in such an orientation. Since the latter is dominated by quantum mechanical tunneling, we are not able to capture it entirely in the present simulations, hence our observed reorientation mechanism is entirely due to rotation. This is illustrated in Fig. 7a, which shows the evolution of the quantity $|\hat{\mathbf{u}}_{NH}(t) - \hat{\mathbf{u}}_{NH}(0)|$, where $\hat{\mathbf{u}}_{NH}(t)$ is the unit vector along a typical NH bond of an ammonia molecule. The trajectory plot gives a qualitative picture of the rotational motion of NH_3. In the initial segment of the trajectory from 0 to about 0.3 ps, the ammonia is hydrogen-bonded to an NH_4^+ ion just after a proton-transfer event. It can be seen that rotational motion is hindered due to the hydrogen bond. At 0.3 ps, the hydrogen bond breaks, and the NH_3 is "free", and a corresponding increase in the rotational activity can be seen from the figure. Despite the limitations of a purely classical treatment of the nuclear motion, we, nevertheless, have been able to obtain very compelling evidence of the possibility of umbrella inversion as a means of NH_3 reorientation in the lattice. This is illustrated by a plot of probability distribution function of the average angle between the three NH bonds and the C_3 axis, which is shown in Fig. 7b. The figure shows that the angle has a broad distribution that often approaches values near 90°. This suggests that a fully quantum mechanical treatment of the nuclear motion via ab initio path integrals [55,56] should be able to capture this phenomenon, if it can occur. As part of future work, we plan to carry out

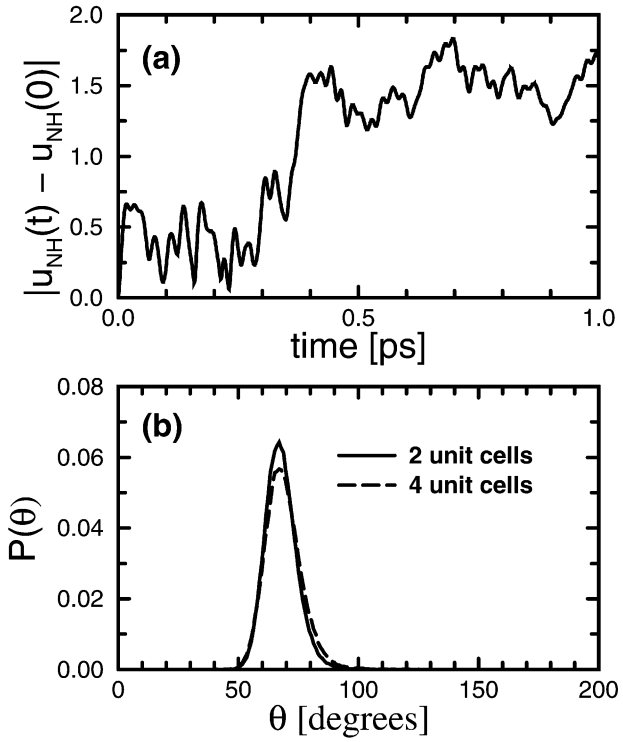

Fig. 7 (a) Typical trajectory of the quantity $|\hat{u}_{NH}(t) - \hat{u}_{NH}(0)|$ for an ammonia molecule as it evolves from participation in a $N_2H_7^+$ complex to "free" after hydrogen-bond breaking in the doped cubic ammonium perchlorate crystal at 530 K. (b) Probability distribution function of the average angle θ between the NH bond vectors and the unit vector along the C_3 axis an NH_3 unit in the doped cubic ammonium perchlorate crystal at 530 K for 2 unit cells (solid line) and 4 unit cells (dashed line).

such ab initio path integral simulations in order to explore how the inclusion of nuclear quantum effects changes the relative importance of rotation vs. umbrella inversion.

CONCLUSIONS

Ab initio molecular dynamics studies of pure ammonium perchlorate crystal in its low-temperature orthorhombic and high-temperature cubic phases have been performed. Additional simulations of ammonium perchlorate crystal doped with neutral ammonia molecules at a 0.5 mole fraction in the cubic phase have also been carried out. The aim of these studies has been to investigate the charge-transport mechanism in both the pure and doped crystals. Infrared spectra extracted from the trajectories show that the NH stretch peak of the pure crystal is broadened into a lower frequency region in the doped crystal, suggesting the formation of strongly hydrogen-bonded $N_2H_7^+$ complexes in the latter system and providing direct, experimentally verifiable evidence for the existence of such complexes. These complexes are also observed directly from the trajectory and indicate that, in the doped crystal, charge transport can occur via a Grotthuss hopping mechanism in which NH_4^+ ions transfer an excess proton to the neutral NH_3 molecules at interstitial sites through the hydrogen bonds in these $N_2H_7^+$ complexes. Rotational mean-square-displacement curves indicate that the newly formed NH_3 molecules undergo rapid reorientation, allowing them to accept protons from other NH_4^+ ions in the lattice. The simulations also show compelling evidence for a possible NH_3 umbrella inversion process that may play a significant role in the charge-transport mechanism. Further exploration of this will require inclusion of nuclear quantum effects and will be deferred for future work. That a marked enhancement in the rate of charge transport is found for the doped crystal compared to the pure crystal is in agreement with experimental observations [7]. Moreover, the ratio of the diffusion constants of NH_4^+ for the doped and pure crystals is in good agreement with the experimentally measured conductivity ratio for these two systems. This finding, together with the fact that no proton transfer events between NH_4^+ and ClO_4^- ions is observed for the pure crystal in the present simulations, suggests that the charge-transport mechanism in the pure crystal is dominated by pure diffusion of NH_4^+, which is rate-limited by the slow diffusion of ClO_4^- ions. Finally, the rotational motion of both types of ions was studied in the pure crystal. It was found, in agreement with experiment, that the NH_4^+ ions undergo nearly free rotation in both phases while rotational diffusion of ClO_4^- ions is noticeably larger in the cubic phase compared to the orthorhombic phase.

The present study underscores the fact that solid-state charge transport can be influenced by a wide variety of dynamical factors. In the present case, translational diffusion is strongly coupled to rotational diffusion of the two types of ions present. When the pure ammonium perchlorate crystal is doped with neutral ammonia, another mechanism comes into play, namely, the Grotthuss proton hopping mechanism via short-lived $N_2H_7^+$ complexes. Given the growing importance of solid-state proton conduction, we hope that the present studies will inspire further theoretical and experimental investigation into the microscopic mechanisms that govern the charge-transport process in molecular crystals.

ACKNOWLEDGMENTS

Most of the calculations performed here were performed on the Lemieux system at the Pittsburgh Supercomputing Center and at the Hewlett-Packard high-performance computing facilities in Richardson, TX. This work has been supported by NSF CHE-9875824, NSF CHE-0121375, and a Research Corporation Research Innovations Award RI0218.

REFERENCES

1. M. E. Tuckerman, K. Laasonen, M. Sprik, M. Parrinello. *J. Phys. Chem.* **99**, 5749 (1995).
2. M. E. Tuckerman, K. Laasonen, M. Sprik, M. Parrinello. *J. Chem. Phys.* **103**, 150 (1995).

3. N. Agmon. *Chem. Phys. Lett.* **244**, 456 (1995).
4. D. Marx, M. E. Tuckerman, J. Hutter, M. Parrinello. *Nature* **367**, 601 (1999).
5. M. E. Tuckerman, D. Marx, M. Parrinello. *Nature* **417**, 925 (2002).
6. T. C. Waddington. *J. Chem. Soc.* **DEC**, 4340 (1958).
7. H. Wise. *J. Phys. Chem.* **71**, 2843 (1967).
8. P. W. M. Jacobs and A. Russel-Jones. *J. Phys. Chem.* **72**, 202 (1968).
9. P. W. M. Jacobs and H. M. Whitehead. *Chem. Rev.* **69**, 551 (1969).
10. E. F. Westrum, Jr. and B. H. Justice. *J. Chem. Phys.* **50**, 5083 (1969).
11. J. W. Riehl, R.Wang, H. W. Bernard. *J. Chem. Phys.* **58**, 508 (1973).
12. L. Glasser. *Chem. Rev.* **75**, 21 (1975).
13. H. J. Prask, S. F. Trevino, J. J. Rush. *J. Chem. Phys.* **62**, 4156 (1975).
14. I. A. Oxton, O. Knop, M. Falk. *J. Mol. Struct.* **37**, 69 (1977).
15. E. F. Khairetdinov and V. V. Boldyrev. *Thermochim. Acta* **41**, 63 (1980).
16. R. M. Corn and H. L. Strauss. *J. Chem. Phys.* **79**, 2441 (1983).
17. P. Colomban and A. Novak. In *Proton Conductors: Solids, Membranes and Gels—Materials and Devices*, Chap. 11, Cambridge University Press, Cambridge (1992).
18. M. F. Foltz and J. L. Maienschein. *Mat. Lett.* **24**, 407 (1995).
19. T. G. Devi, M. P. Kannan, B. Hema. *Thermochim. Acta.* **285**, 269 (1996).
20. A. L. Ramaswamy, H. Shin, R. W. Armstrong. *J. Mater. Sci.* **31**, 6035 (1996).
21. W. L. Elban and R. W. Armstrong, *Acta Mater.* **17**, 6041 (1998).
22. S. M. Peiris, G. I. Pangilinan, and T. P. Russel. *J. Phys. Chem. A* **104**, 11188 (2000).
23. J. M. Winey, Y. A. Gruzdkov, Z. A. Dreger, B. Jensen, Y. M. Gupta. *J. Appl. Phys.* **91**, 5650 (2002).
24. D. W. Oxtoby, H. P. Gillis, N. H. Nachtrieb. *Principles of Modern Chemistry*, Saunders College Publishing, Fort Worth, TX (1999).
25. R. Car and M. Parrinello. *Phys. Rev. Lett.* **55**, 2471 (1985).
26. M. Diraison, G. J. Martyna, M. E. Tuckerman. *J. Chem. Phys.* **111**, 1096 (1999).
27. Y. Liu and M. E. Tuckerman. *J. Phys. Chem. B* **105**, 6598 (2001).
28. L. Jaroszewski, B. Lesyng, J. J. Tanner, J. A. McCammon. *Chem. Phys. Lett.* **175**, 282 (1990).
29. L. Jaroszewski, B. Lesyng, J. A. McCammon. *J. Mol. Struct.* **283**, 57 (1993).
30. J. A. Platts and K. E. Laidig. *J. Phys. Chem.* **99**, 6487 (1995).
31. B. S. Jursic. *J. Mol. Struct.* **393**, 1 (1997).
32. T. Asada, H. Haraguchi, K. Kitaura. *J. Phys. Chem. A* **105**, 7423 (2001).
33. W. Buessem and H. Herrmann. *Z. Kristallogr.* **74**, 458 (1930).
34. K. Venkatesan. *Proc. Indian Acad. Sci.* **46A**, 134 (1957).
35. H. G. Smith and H. A. Levy. *Acta Cryst.* **15**, 1201 (1962).
36. K. Herrmann and W. Ilge. *Z. Kristallogr.* **75**, 31 (1930).
37. A. D. Becke. *Phys. Rev. A* **38**, 3098 (1988).
38. W. Y. C. Lee and R. C. Parr. *Phys. Rev. B* **37**, 785 (1988).
39. N. Troullier and J. L. Martins. *Phys. Rev. B* **43**, 1993 (1991).
40. S. Goedecker, M. Teter, J. Hutter. *Phys. Rev. B* **54**, 1996 (1996).
41. C. Hartwigsen, S. Goedecker, J. Hutter. *Phys. Rev. B* **58**, 1998 (1998).
42. A. K. Soper, F. Bruni, M. A. Ricci. *J. Chem. Phys.* **106**, 247 (1997).
43. G. J. Martyna, M. E. Tuckerman, M. L. Klein. *J. Chem. Phys.* **97**, 2635 (1992).
44. J. Hutter, A. Alavi, T. Deutsch, M. Bernasconi, S. Goedecker, D. Marx, M. Parrinello, M. E. Tuckerman. CPMD Version 3.3, Max-Planck Institut fuer Festkoerperforschung and IBM Zurich Research Laboratory, 1995–1999.
45. M. E. Tuckerman, D. A. Yarne, S. O. Samuelson, G. J. Martyna. *Comp. Phys. Commun.* **128**, 333 (2000).
46. R. D. King-Smith and D. Vanderbilt. *Phys. Rev. B* **47**, 1651 (1993).

47. R. Resta. *Rev. Mod. Phys.* **66**, 899 (1994).
48. P. L. Silvestrelli, M. Bernasconi, M. Parrinello. *Chem. Phys. Lett.* **277**, 478 (1997).
49. R. Resta. *Phys. Rev. Lett.* **80**, 1800 (1998).
50. R. Resta. *J. Phys. Condens. Matter* **14**, R625 (2002).
51. B. Guillot. *J. Chem. Phys.* **95**, 1543 (1991).
52. W. Nailong. *The Maximum Entropy Method*, Springer, Berlin (1997).
53. Z. Zhu and M. E. Tuckerman. *J. Phys. Chem. B* **106**, 8009 (2002).
54. J. L. Atwood, L. J. Barbour, A. Jerga. *J. Am. Chem. Soc.* **124**, 2122 (2002).
55. D. Marx and M. Parrinello. *J. Chem. Phys.* **104**, 4077 (1996).
56. M. E. Tuckerman, D. Marx, M. L. Klein, M. Parrinello. *J. Chem. Phys.* **104**, 5579 (1996).